Molecular Cell, Vol. 8, 1363–1373, December, 2001, Copyright ©2001 by Cell Press

The Nucle(ol)ar Tif6p and Efl1p Are Required for a Late Cytoplasmic Step of Ribosome Synthesis

Bruno Senger,[1] Denis L.J. Lafontaine,[3] Jean-Sebastien Graindorge,[1] Olivier Gadal,[4] Alain Camasses,[2] Ambaliou Sanni,[1] Jean-Marie Garnier,[5] Michael Breitenbach,[6] Eduard Hurt,[4] and Franco Fasiolo[1,7]

[1]UPR n° 9002 du CNRS
[2]UPR n° 9005 du CNRS
Institut de Biologie Moleculaire et Cellulaire du CNRS
15 Rue Rene Descartes
67084 Strasbourg Cedex
France
[3]FNRS
Institut de Biologie et de Médecine Moléculaires
Unitersité Libre de Bruxelles
Rue des Professeurs Jeener et Brachet 12
B-6041 Charleroi-Gosselies
Belgium
[4]BZH, Biochemie-Zentrum Heidelberg
Im Neuenheimer Feld 328
D-69120 Heidelberg
Germany
[5]Institut de Genetique et de Biologie Moleculaire et Cellulaire
67404 Illkirch
France
[6]Department of Genetics
Salzburg University
Hellbrunnerstrasse 34
A-5020 Salzburg
Austria

Summary

Deletion of elongation factor-like 1 (Efl1p), a cytoplasmic GTPase homologous to the ribosomal translocases EF-G/EF-2, results in nucle(ol)ar pre-rRNA processing and pre-60S subunits export defects. Efl1p interacts genetically with Tif6p, a nucle(ol)ar protein stably associated with pre-60S subunits and required for their synthesis and nuclear exit. In the absence of Efl1p, 50% of Tif6p is relocated to the cytoplasm. In vitro, the GTPase activity of Efl1p is stimulated by 60S, and Efl1p promotes the dissociation of Tif6p-60S complexes. We propose that Tif6p binds to the pre-60S subunits in the nucle(ol)us and escorts them to the cytoplasm where the GTPase activity of Efl1p triggers a late structural rearrangement, which facilitates the release of Tif6p and its recycling to the nucle(ol)us.

Introduction

Ribosome biogenesis involves the synthesis, maturation, and assembly of ribosomal RNAs (rRNAs) and ribosomal proteins (r-proteins). In eukaryotes, three out of the four rRNAs (5.8S, 18S, and 25S rRNAs) are interspersed with noncoding sequences in a single, large precursor from which they are released following a complex processing pathway involving both endo- and exonucleolytic digestions (reviewed in Kressler et al. 1999; Venema and Tollervey, 1999). Concomitantly, pre-rRNAs are extensively modified by base and ribose methylation and formation of pseudouridine residues and are bound by the r-proteins (reviewed in Woolford and Warner, 1991; Raué and Planta, 1991). R-proteins are synthesized in the cytoplasm and need to be specifically targeted to the nucleolus where most steps of ribosomal assembly occur. In the course of assembly, pre-ribosomes are exported to the cytoplasm and undergo late and ill-defined steps of maturation before they engage in translation (Warner, 1971; Trapman and Planta, 1976). Altogether, this represents a major metabolic activity for the cells (Warner, 1999).

The mechanisms of ribosome export are not very well characterized. Pioneering work, based on coinjection experiments in *Xenopus* oocytes, demonstrated that ribosome export is a unidirectional, saturable, and energy-dependent process (Bataille et al. 1990). Recently, two assays have been reported in yeast to follow the nuclear exit of ribosomes (Hurt et al. 1999; Moy and Silver, 1999). From this, it was concluded that ribosome export is dependent on a subset of nucleoporins and the small GTPase Ran. Yeast genetics is now leading to the identification of the first *trans*-acting factors specifically required for ribosome export. Rpl10p, a protein that joins the large ribosomal subunit late in the assembly pathway, is bound by Nmd3p, which acts as a nuclear export signal (NES)-containing adaptor for the export receptor Xpo1p/Crm1p (Ho et al. 2000; Gadal et al. 2001). Recently, the Noc proteins found in two subcomplexes (Noc1p-Noc2p and Noc2p-Noc3p enriched in the nucleolus and in the nucleoplam, respectively) and associated with distinct pre-rRNP particles have been shown to be involved both in intranuclear movements and nuclear exit of the ribosomes (Milkereit et al. 2001).

A large number of *trans*-acting factors are involved in pre-rRNA processing, pre-rRNA modification, and ribosomal assembly (Kressler et al. 1999; Venema and Tollervey, 1999). So far, close to 100 factors have been identified. These belong to several families: endo- and exoribonucleases, small nucle(ol)ar ribonucleoprotein particles (snoRNPs), modification enzymes, putative ATP-dependent RNA helicases, and the so-called "chaperones" or "assembly factors" for which the precise function in ribosome synthesis is not known. One such *trans*-acting factor is Tif6p, an essential nucle(ol)ar yeast protein showing homology to the mammalian translation factor eIF6 (Si et al. 1997; Sanvito et al. 1999; Si and Maitra, 1999; Wood et al. 1999). Despite its homology to eIF6, Tif6p is not required for translation. In fact, cells depleted for Tif6p are defective for 5.8S and 25S rRNA synthesis (Basu et al. 2001) and consequently strongly underaccumulate 60S subunits (Sanvito et al. 1999; Si and Maitra, 1999; Wood et al. 1999; Basu et al. 2001). In vitro, Tif6p binds to the large ribosomal subunit and prevents its association with the 40S subunits (Si and

[7]Correspondence: f.fasiolo@ibmc.u-strasbg.fr

Maitra, 1999); the biological significance of this observation is not clear at present.

Eukaryotic ribosome synthesis relies on extensive structural rearrangements, and no less than 17 different putative ATP-dependent RNA helicases have been involved in this process so far (de la Cruz et al. 1999). The large majority of rRNA modification is mediated by a class of highly conserved, small nucle(ol)ar RNAs (snoRNAs) and their associated proteins (reviewed in Lafontaine and Tollervey, 1998). Sites of modification are specifically selected by Watson-Crick (W-C) base pair interactions between the snoRNAs and the pre-rRNAs. With an estimated 200 different snoRNAs showing up to 21 consecutive nucleotides of perfect complementarity to the pre-rRNAs, the need for structural isomerization is very important. Other snoRNAs are involved in pre-rRNA processing rather than modification, but their function also involves W-C base pairing with the pre-rRNAs. Structural rearrangements are also expected to be required to generate pre-rRNP substrates competent for cleavage and binding of *trans*-acting factors and ribosomal proteins.

In the mature ribosome, conformational changes are mediated by another class of highly conserved proteins, the GTPases EF-Tu and EF-G (EF1α and EF-2 in eukaryotes, respectively). Hydrolysis of EF-Tu-GTP to EF-Tu-GDP and Pi delivers an aminoacyl-tRNA to the A-site; GTP hydrolysis by EF-G induces a large-scale rearrangement of the tRNA-mRNA-ribosome complex during translocation (reviewed in Nygard and Nilsson, 1990; Lafontaine and Tollervey, 2001). In addition to their essential function in translation, G-proteins are involved in most key cellular processes, including signal transduction and cell proliferation, cytoskeletal organization, vesicular transport, nucleo-cytoplasmic transport, and pre-mRNA splicing (U5-116 kDa/yeast Snu114p) (Fabrizio et al., 1997). Surprisingly, no G protein has been involved in ribosome synthesis so far.

Here we report the identification and functional characterization of Efl1p, a cytoplasmic GTPase highly homologous to the elongation factors EF-G/EF-2, which is required for ribosome synthesis.

Results

Efl1p Is a G-Domain Containing Protein Homologous to the Ribosomal Translocases EF-G and EF-2

EFL1 (Elongation Factor-Like 1) was fortuitously cloned by PCR using degenerated oligonucleotides against a conserved domain of a yeast aminoacyl-tRNA synthetase that amplified a 72 base pair fragment of DNA homologous to the GTP domain of *Dictyostelium discoideum* EF-2. Sequence comparison of the entire *EFL1* coding sequence (YNL163c) with available EF-2 and EF-G sequences allowed the construction of a phylogenetic tree showing that Efl1p is homologous to the eukaryotic and archaebacterial ribosomal translocases (Figure 1B). The comparison with EF-G from *T. thermophilus* (Figure 1A) (Aevarsson et al. 1994) revealed that Efl1p has the basic organization of a translocation factor composed of the G domain (domain I) and domains II–V. The G domain that binds and hydrolyses GTP consists of five highly conserved motifs (Figure 1A, boxes G1–G5). Both the relative position of the boxes within the G domain and the residues known from the crystal structures to be involved in the interactions with GTP are conserved in Efl1p (Figure 1A) (Berchtold et al. 1993; Czworkowski et al. 1994). Typically, the presence of the conserved aspartate 121 and arginine 588 characteristic of the G domain fingerprint amino acids (Aevarsson, 1995), underline the putative GTPase activity of Efl1p. A distinguishing feature of Efl1p is the presence of a 160 amino acid insertion between the G domain and domain II that has no equivalent among other EF-2-like factors (indicated in yellow in Figure 1A); 40% of this insertion consists of small stretches of acidic/serine residues. Deletion of the insertion domain results in a thermosensitive phenotype (our unpublished data). Homologs of Efl1p are present in *Homo sapiens*, *Arabidopsis thaliana*, *Drosophila melanogaster*, and *Schizosaccharomyces pombe*, indicating that the protein is highly conserved.

Deletion of *EFL1* Confers a Severe Slow Growth Phenotype

To assess the function of Efl1p in vivo, an internal 2 kb StuI fragment of *EFL1* (YNL163C) was replaced by the selective marker HIS3 and the disrupted allele (*efl1*Δ*1*) introduced by homologous recombination in the genome of yeast YPH501 diploid strain. In *efl1*Δ*1*, a portion of the G-domain, the 160 amino acid insertion, and domains II–IV are deleted (Figure 1A, underlined). Tetrad analysis yielded two spores (His^-) with wild-type growth rates and two spores (His^+) with severe slow growth phenotype. This indicated that *EFL1* was not essential for spore germination or growth. *efl1*Δ*1* haploid strains showed a doubling time of $\sim$10 hr on complete medium (compared to 2 hr for the wild-type control) and could be fully complemented for growth by an intact copy of *EFL1* present on a low-copy (ARS/CEN) plasmid (data not shown). No stable product was detected in the *efl1*Δ*1* allele by Western blotting using a polyclonal antibody raised against recombinant Efl1p (data not shown). A full deletion of *EFL1* demonstrated that the gene is indeed not essential, and strains with a null *efl1* allele showed a doubling time similar to that of *efl1*Δ*1* strains (data not shown). In this report, the function of Efl1p was characterized in *efl1*Δ*1* strains.

Efl1p Is a Cytoplasmic Protein

Efl1p was fused to GFP and visualized in live cells by fluorescence microscopy. The GFP-Efl1p fusion was fully functional as shown by its ability to complement for growth *efl1*Δ*1* strains (data not shown). GFP-Efl1p was absent from vacuoles and nuclear regions and produced a fluorescence pattern consistent with a predominantly cytoplasmic localization (Figure 1C).

The cellular distribution of Efl1p was also addressed by subcellular fractionation. Highly enriched nuclear and cytoplasmic fractions were prepared from whole-cell lysates (as described in Galy et al. 2000) and analyzed by SDS-PAGE and Western blotting. This confirmed that Efl1p is a cytosolic protein (Figure 1D). As a control for the cell fractionation, membranes were probed for valyl-tRNA synthetase, which is cytoplasmic.

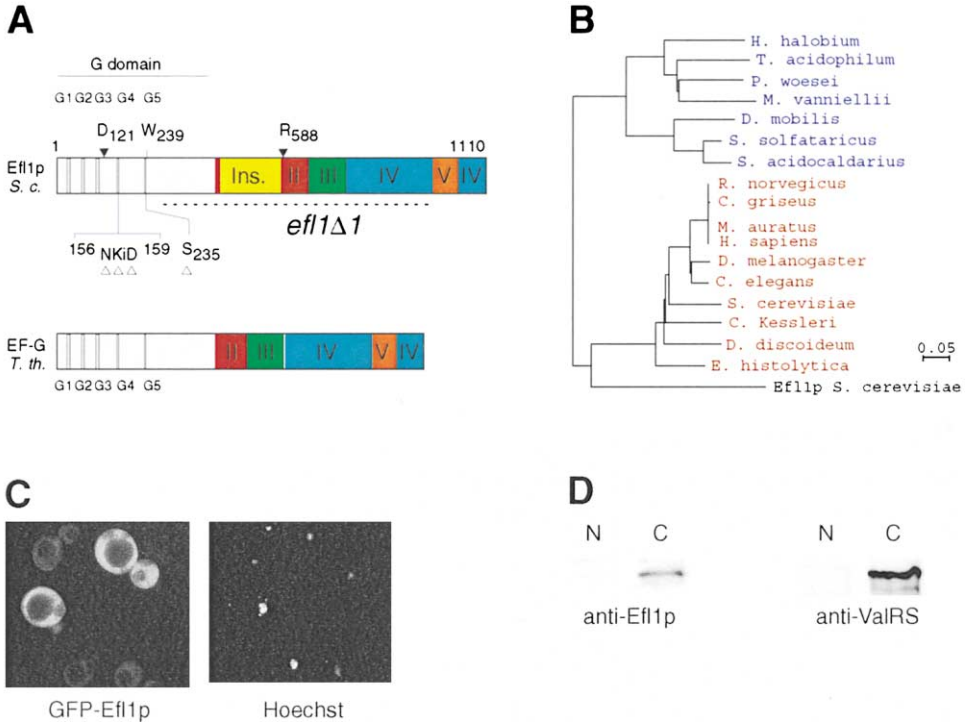

Figure 1. Efl1p Is a Cytoplasmically Located G Protein Homologous to the Family of EF-2/EF-G Translocases

(A) Diagram of the primary structure of Efl1p from *S. cerevisiae*. The five domains defined by the crystal structure of EF-G from T. thermophilus (Aevarsson et al. 1994; Czworkowski et al. 1994) are color coded as follows: domain I (G domain in black), domain II (red), domain III (green), domain IV (blue), and domain V (orange). Open arrowheads indicate functional residues from the G4 and G5 boxes that are involved in guanine base recognition (Berchtold et al. 1993; Czworkowski et al. 1994). Closed arrowheads indicate conserved amino acids involved in salt bridge formation between domains I and II (Aevarsson, 1995). The highlighted tryptophan (position 239 in Efl1p) was found to be important for the interaction with the ribosomal RNA sarcin/ricin loop (Aevarsson, 1995).

The 160 amino acid insertion within domain II is indicated in yellow. The domain of Efl1p that is replaced by the HIS3 marker in *efl1Δ1* strain is underlined.

No truncated Efl1p product was detected in the *efl1Δ1* strain using anti-GST-Efl1p antibodies.

(B) Phylogenetic tree derived from the alignment of 17 eukaryotic EF-2 and archaebacterial EF-G ribosomal translocases using with PileUp (GCG package version 9. 1) Ribosomal translocases from Archaea, and eukaryotes are represented in blue and in red, respectively. Efl1p is indicated in black. The unrooted phylogenetic tree was obtained using the Bootstrap Neighbor-Joining tree option incorporated in the ClustalX 1. 81 Package (1000 bootstrap replicates were performed). The number indicates the degree of divergence.

(D) Fluorescence microscopic localization of GFP-Efl1p and subcellular distribution of wild-type Efl1p.

GFP-tagged Efl1p was expressed in *efl1Δ1* using a pRS315-derived pNOP1-GFP plasmid (CEN/LEU). The GFP signal was examined in the fluorescein channel of a Zeiss Axioskop fluorescence microscope. GFP-Efl1p showed a cytoplasmic fluorescence signal with vacuolar and nuclear exclusion (left panel). Hoechst 33342, UV channel indicating the position of the nuclei (right panel).

(D) Cell fractionation. The procedure for the cell fractionation is described in Galy et al. (2000). Immunoblots of nuclear and cytoplasmic fractions from wild-type yeast cells using anti-GST-Efl1p antibodies (left panel) and anti-valyl-tRNA synthetase (ValRS) antibodies as a control (right panel) are shown. Crude cytosolic protein extract from about 0.3 A_{600} cells was loaded on lane C (cytoplasmic). Equivalent amounts of nuclear protein extracts were loaded on lane N (nuclear). Efl1p and ValRS were visualized using the ECL protocol (Amersham) and corresponding specific sera diluted 1/2500 and 1/1000, respectively.

efl1Δ1 Strains Underaccumulate 60S Ribosomal Subunits

The homology to translation factors and the cytoplasmic localization of Efl1p suggested a possible role in ribosome function. This prompted us to test whether Efl1p is associated with mature ribosomes and to analyze polyribosome profiles by sucrose density gradient centrifugation as described (Wood et al., 1999).

The wild-type strain (YPH500) showed a typical polysomal profile with free 40S and 60S subunits, 80S monosomes, and higher order polysomal fractions (Figure 2A). Total protein was extracted from selected fractions of the gradient, separated by SDS-PAGE, and transferred to nitrocellulose membranes. Western blot hybridization with Efl1p-specific antibodies revealed that the protein is not associated with any of the ribosomal fractions. Rather, Efl1p was found at the top of the gradient, most likely as a soluble protein (Figure 2B, fractions 30 and 31).

Analysis of ribosomal fractions from *efl1Δ1* strains revealed a drastic decrease in the number of polyribosomes and a marked imbalance in the 60S to 40S subunits ratio (Figure 2C). This suggested impairment in the synthesis and/or stability of the large ribosomal subunit rather than an inhibition of translation. To quantify the relative amounts of 60S versus 40S, gradients were run in the presence of 800 mM KCl. Under these conditions, 60S and 40S subunits are dissociated (Si and Maitra,

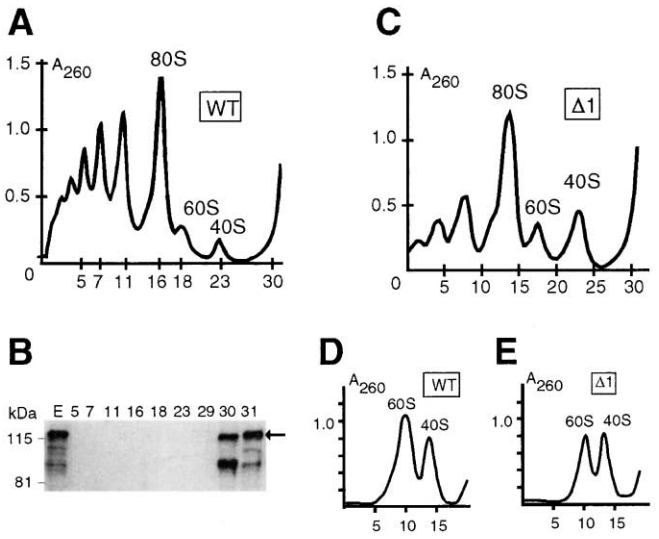

Figure 2. *Efl1*-Deficient Strains Underaccumulate Large Ribosomal Subunits but the Protein Is Not Associated with the Ribosomes

(A) Sucrose gradient analysis of polyribosome profile from cycloheximide-arrested wild-type (A) (YPH500) and *efl1Δ1* (C) (JS544-6A) cells.

(B) Western blot analysis of fractions presented in (A) using anti-GST-Efl1p antibodies (1/5000 dilution of the serum).

The arrowhead represents the position of the native Ef1p in the fractions and in the crude protein extract (lane E). Sucrose gradient analysis of subunits content in dissociation conditions (800 mM KCl) for the wild-type (D) and the *efl1Δ1* (E) strains is shown.

1999). This analysis confirmed the strong subunit imbalance. For the wild-type strain, the 60S to 40S ratio gave a standard value of ~2 (Figure 2D), reflecting a 1:1 stoichiometry. In *efl1Δ1* strains, this ratio was only about 1 (Figure 2E), reflecting the underaccumulation of 60S subunits.

efl1Δ1 Strains Are Defective for Pre-rRNA Processing

To test whether the ribosomal subunits' imbalance observed in *efl1*-deficient strains could result from defects in pre-rRNA processing, total RNA was extracted from *efl1Δ1* and wild-type isogenic strains and analyzed by Northern blot hybridization, primer extension, and pulse-chase analysis.

Three out of the four eukaryotic rRNAs, 5.8S, 18S, and 25S rRNAs, are produced from a single large Pol I precursor (35S pre-rRNA in yeast) by successive endo- and exonucleolytic digestions (Figure 3A). Hybridization with oligonucleotides specific to the mature rRNAs revealed that while the steady-state level of the 18S rRNA was not greatly affected in *efl1Δ1* strains, the accumulation of the 5.8S and 25S rRNAs was substantially reduced (Figure 3B, lanes 1 and 2). Phosphor Imager quantitation estimated this reduction to be ~40% of their wild-type counterparts. As loading controls, membranes were probed specifically for 5S rRNA, which is processed independently from a Pol III transcript.

In wild-type yeast strains, the 35S pre-rRNA is cleaved successively at sites A_0 and A_1 in the 5′ external transcribed spacer (5′-ETS) and at site A_2 in the internal transcribed spacer 1 (ITS1), generating the 33S, 32S, and $27SA_2$ and 20S pre-rRNAs (Figures 3A and 3B, lanes 3, 5, 7, and 9). In *efl1Δ1* strains, early pre-rRNA processing reactions at sites A_0, A_1, and A_2 appeared severely delayed leading to the accumulation of the 35S pre-rRNA (Figure 3B lanes 4, 6, 8, and 10). In the absence of processing at sites A_0–A_2, the 35S pre-rRNA was first cleaved at site A_3 in ITS1 generating an aberrant 23S RNA and the $27SA_3$ pre-rRNA. The 23S RNA extends from the site +1 of transcription to site A_3 and is only detected with oligonucleotides specific to sequences upstream of A_3, i.e., with oligonucleotides b and c, but not with oligonucleotides d or e (Figure 3B).

Despite the strong accumulation of 23S RNA, cleavages at sites A_0, A_1, and A_2 were kinetically delayed rather than fully inhibited and a substantial residual level of $27SA_2$ and 20S pre-rRNA was synthesized (Figure 3B, lanes 3–6). This residual level of wild-type pre-rRNA processing was apparently sufficient to produce levels of 18S similar to those of wild-type strains (Figure 3B, lanes 1 and 2). Alteration in the kinetics of early pre-rRNA processing was also illustrated by the accumulation of 33S pre-rRNA (specifically detected with oligo g, data not shown), which is not normally detected by Northern blot due to its low abundance and low levels of an aberrant 22S RNA (Figure 3B, lane 6 and inset) extending from site A_0 to site A_3.

The efficiency of cleavage at site A_3 was specifically tested by primer extension. cDNAs were extended across ITS1 from oligonucleotide e allowing specific detection of RNA species with 5′ ends at sites A_2, A_3, and B_1 (Figure 3C). As expected from the strong accumulation of 23S RNA, cleavage at site A_3 did not appear to be affected in *efl1Δ1* strains (Figure 3C). However, the signal at site B_1 was strongly increased. Northern blot hybridization with oligonucleotide e, complementary to the 5′-end of ITS2, revealed that this increased signal at site B_1 corresponded to a strong accumulation of 27SB pre-rRNAs (Figure 3B lanes 9 and 10) indicating that downstream processing at sites $C_2 \rightarrow C_1$ is severely inhibited in *efl1Δ1* strains. This is responsible for the underaccumulation of 7S pre-rRNA and 5.8S and 25S rRNAs (Figure 3B, lanes 1 and 2). The reduction of cleavage at site A_2 reported by Northern blot was also confirmed by this analysis (Figure 3C).

Primer extension was similarly performed across the 5′-ETS from oligonucleotide a complementary to the 5′-end of 18S rRNA (Figure 3A). In agreement with the accumulation of 35S and 23S RNAs detected by Northern blot, the signal corresponding to site +1 was substantially increased in *efl1Δ1* strains (Figure 3C). Similarly, the increase of the signal at A_0 is fully consistent with the higher levels of 33S pre-rRNA and 22S RNA in the mutant strain (Figure 3B, lane 6). In vivo pulse-

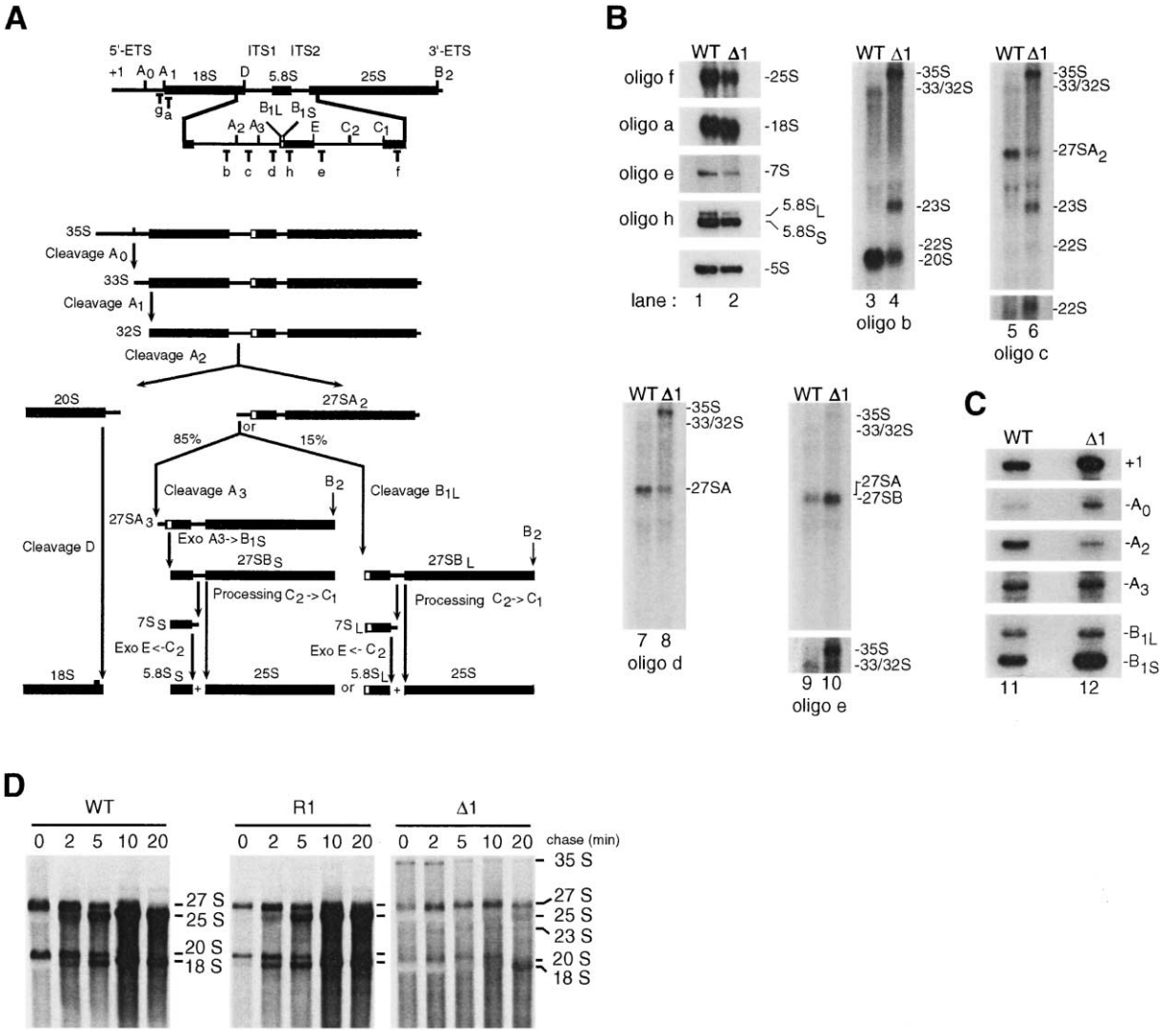

Figure 3. Efl1p Is Required for Pre-RNA Processing

(A) Structure of the rDNA operon and location of the oligonucleotides used in this work. The mature 18S, 5.8S, and 25S rRNAs (bold lines) are released from the 35S primary transcript following cleavages in the external transcribed spacers (5′- and 3′-ETS) and internal transcribed spacers (ITS1 and ITS2). Cleavage sites are indicated by upper case letters (A_0–D). Oligonucleotides used for the Northern blot hybridization and primer extension experiments are indicated in lower case (a–h).

Pre-rRNA processing pathway (lower part of the figure and right panel) is shown. The pre-rRNA processing steps and different processing intermediates are indicated (adapted from Venema and Tollervey, 1999).

(B) Northern analysis (lanes 1–10).

(C) Primer extension was performed from oligonucleotide a (for specific detection of RNAs with 5′ ends corresponding to sites +1 and A_0) and oligonucleotide e (for sites A_2, A_3, B_{1L}, and B_{1S}).

(D) Pulse-chase labeling analysis of pre-RNA processing in (WT, YPH500), *efl1Δ1* strain (JS544-6A), and R1(JS544-6A R1) strains. Cells were labeled with [^{3}H]-uracil for 2 min and chased with an excess of unlabeled uracil for 2, 5, 10, and 20 min as indicated. The positions of 35S, 27S, 25S, 23S, 20S, and 18S rRNA are indicated.

chase labeling analysis further confirmed the kinetic delay in the synthesis of both 25S and 18S rRNAs in *efl1*-deficient strains and the greater deficiency of 25S rRNA relative to 18S rRNA (Figure 3D).

The cytoplasmic distribution of Efl1p appeared in contradiction with its involvement in nucle(ol)ar pre-rRNA processing. To investigate the possibility that the protein shuttles between the nucleus and the cytoplasm, the distribution of the GFP-Efl1p fusion was tested in mutant strains known to either shut the nuclear pore complexes (NPC) or affect nucleo-cytoplasmic exchanges. Strains tested included *xpo1-1*, *xpo1*-LMB, *rna1*, *prp20-1*, *nmd3-2*, *rpl10-1*, *nsp1-5*, *nic96-1*, and *dis3-1* (Gadal et al., 2001 and references therein). None of these mutants showed a significant nuclear accumulation of GFP-Efl1p when tested in nonpermissive conditions (data not shown). This suggested an indirect involvement of Efl1p in ribosome synthesis.

Efl1p Interacts Genetically with Tif6p

The slow growth phenotype of *efl1Δ1* strains was used to screen for extragenic and multicopy suppressors.

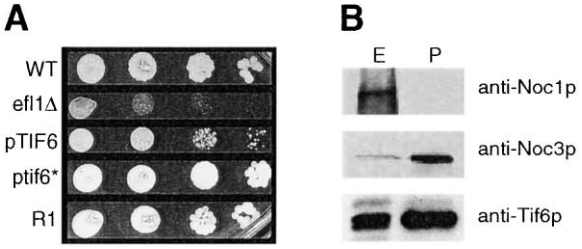

Figure 4. Genetic Interactions between Efl1p and Tif6p and Association of Tif6p with 60S Pre-Ribosomal Particles

(A) Complementation of slow growth phenotype in *efl1*-deficient strain. Drop test assay was performed at 25°C on synthetic minimal. Left to right, serial dilutions (1×–10^3×). Top to bottom: wild-type control (WT, YPH500), *efl1Δ1* strain (JS544-6A), *efl1Δ1* transformed with a low copy plasmid expressing TIF6 (pTIF6), *efl1Δ1* transformed with a low copy plasmid expressing tif6* (ptif6*), and original revertant strain (JS544-6A R1).

(B) Purified 60S pre-ribosomal particles were isolated by tandem affinity purification of Nug1p-TAP according to Bassler et al. (2001). Purified Nug1p (P) and a whole cell lysate (E) were analyzed by SDS-polyacrylamide gel electrophoresis and Western blottig using the indicated antibodies. Note that Noc3p and Tif6p, but not Noc1p, are enriched in the 60S pre-ribosomal particle.

Spontaneous suppressors of the *efl1Δ1* mutant were obtained at a frequency of $\sim 10^{-7}$. Five clones (R1–R5) were selected for further analysis. Standard yeast genetic techniques demonstrated that mutations in these strains are dominant, map to a single gene (show a 2:2 segregation pattern), and belong to a single complementation group (i.e., the same gene is affected in all cases) (see Experimental Procedures). In R1 strains, the growth rate (Figure 4A), the pre-rRNA processing (Figure 3D), the polysome profile, and 60S to 40S ratio (data not shown) were essentially identical to those observed in wild-type strains. A genomic library constructed from strain R1 was transformed in the original *efl1Δ1* strain and screened for complementation of the slow growth phenotype. The suppressor activity was found to lie in an essential gene, *TIF6*. Tif6p is a nucle(ol)ar protein stably associated with 60S subunits and required for 5.8S and 25S rRNA synthesis (Si et al. 1997; Si and Maitra, 1999; Basu et al. 2001). Sequencing of the suppressor allele (tif6*) revealed a single G to T transition changing a valine to a phenylalanine at position 192 (V192F).

In parallel, an *efl1Δ1* strain auxotroph for leucine (JS544-6A) was transformed by a yeast genomic library established in a pUN100-LEU/CEN vector. Fast and slow growing Leu^+ transformants were recovered. Fast growing yeast colonies all carried a plasmid expressing an intact copy of *EFL1*. Three slow growing colonies carried a common 2.8 kb EcoRI fragment from chromosome XVI corresponding to *TIF6* gene flanked by YPR015C and DSS4. Further subcloning analysis mapped the suppressor activity to *TIF6*. R1 strains, and *efl1Δ1* transformed with the tif6* allele (V192F) were nearly completely suppressed for growth. In comparison, *efl1Δ1* strains transformed with pUN100-*TIF6* were only partially complemented for growth (Figure 4A, compare pTIF6 and ptif6* panels).

In conclusion, the slow growth phenotype reported in *efl1Δ1* strains could either be suppressed by a point mutation in Tif6p (tif6* allele) or by mild overexpression of Tif6p. This genetic evidence suggest the existence of functional interactions between Efl1p and Tif6p. The inhibitions in pre-rRNA processing described here for Efl1p-deficient strains are very similar to those reported in strains depleted for Tif6p (Basu et al. 2001). However, Western blot analysis revealed that Efl1p is not simply required for the accumulation of Tif6p (data not shown).

Our attempts to detect physical interactions between Efl1p and Tif6p either in vitro, with recombinant His-tagged versions of the two proteins, or in vivo, in pull-down experiments with either GST- or poly-His-tagged versions of Efl1p, were unsuccessful (data not shown). Presently, it is therefore unclear whether these two proteins interact directly or are organized in a larger pre-rRNP particle. For Tif6p, we found that the protein is associated with late nuclear 60S pre-ribosomes ready to exit the nucleus (for the purification of these particles see Bassler et al. 2001). Indeed, Western blotting revealed that late 60S pre-ribosomes are enriched in both Tif6p and the nucleoplasmic Noc3p, but do not contain Noc1p (Figure 4B), which is restricted to the nucleolus (Milkereit et al. 2001).

Strains Deficient for Efl1p or Tif6p Accumulate the 60S Subunit Reporter Rpl25-eGFP inside the Nucleus

Recently, an assay was reported which allows monitoring of the nuclear export of 60S ribosomal subunits in vivo (Hurt et al. 1999, Gadal et al. 2001). For this, a ribosomal protein from the large subunit (Rpl25p) was fused to GFP (eGFP). In wild-type strains, Rpl25p-eGFP is efficiently incorporated into 60S subunits and is exclusively detected in the cytoplasm by fluorescence microscopy (Figure 5A) (Gadal et al. 2001).

To test whether Tif6p is involved in ribosome export, thermosensitive conditional alleles of *TIF6* were created by random PCR mutagenesis. One of them, *tif6-1*, showed a severe growth defect at 37°C (data not shown) and was used for further analysis. The cellular distribution of Rpl25p-eGFP was assessed in *tif6-1* strains following a shift to 37°C for 8 hr. This revealed a strong nuclear accumulation of Rpl25p-eGFP (Figure 5A).

Similarly, *efl1Δ1* strains were transformed with Rpl25p-eGFP. Like for *tif6-1* strains, *efl1*-deficient strains showed nuclear accumulation of Rpl25p-eGFP (Figure 5A). For comparison, we used a strain expressing a carboxyl truncation of Nmd3p (*nmd3ΔNES1*), which is impaired in large ribosomal subunit export (Figure 5A) (Gadal et al. 2001). It is interesting to note that for all three strains, *tif6-1*, *efl1Δ1*, and *nmd3ΔNES1*, the Rpl25p-eGFP large subunit reporter accumulated throughout the entire nucleus. This suggests that nuclear export is blocked at a late stage, after the release of the pre-ribosomes from the nucleolus (see also Gadal et al. 2001; Milkereit et al. 2001).

The nuclear accumulation of Rpl25p-eGFP in *efl1Δ1* strains was not simply due to its severe slow growth phenotype as an unrelated slow growing strain (deleted for the RNA component of the signal recognition particle) showed no nuclear accumulation of Rpl25p-eGFP (Figure 5A).

Strains showing a nuclear accumulation of Rpl25p-eGFP were further tested for nucle(ol)ar integrity. For this, a DsRed-Nop1p fusion was used as a nucle(ol)ar

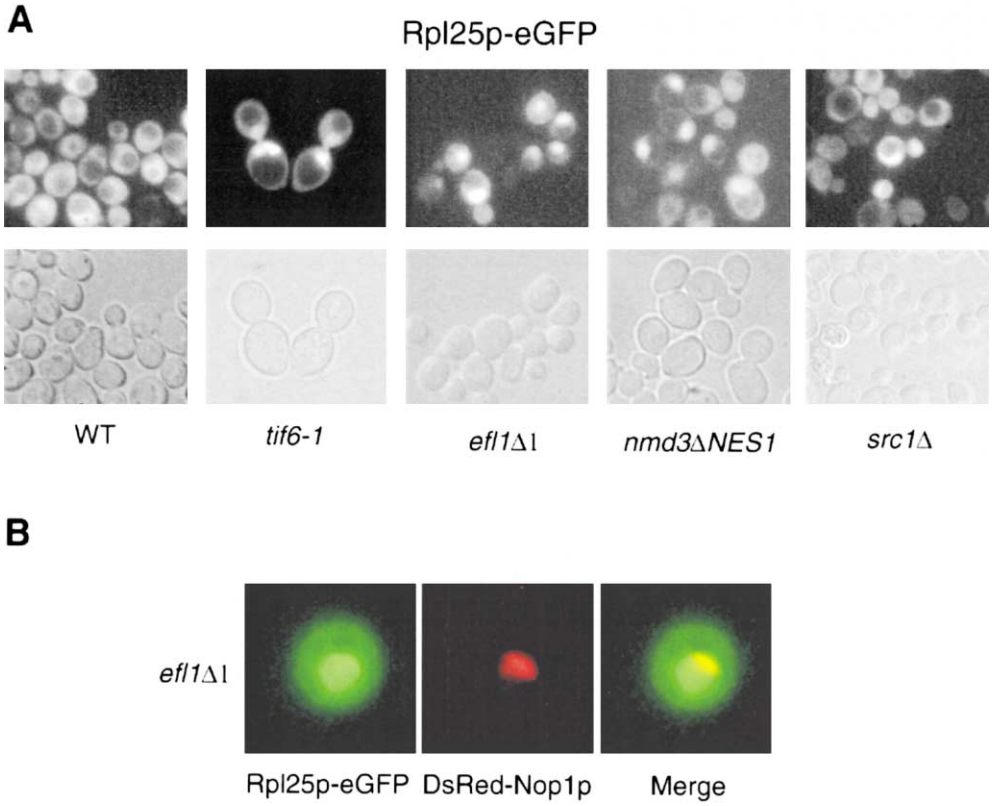

Figure 5. Tif6p and Efl1p Are Required for Ribosome Export

(A) Location of Rpl25p-eGFP in wild-type, *tif6-1*, *efl1Δ1*, *nmd3ΔNES1*, and *src1Δ* mutants. Strains were transformed with Rpl25p-eGFP (pRS315-RPL25-eGFP) and grown at 23°C. The location of the green fluorescent reporter protein was analyzed in the fluorescence microscope. Upper panels: Rpl25p-eGFP accumulates in the nucleoplasm of the slow growing mutant *efl1Δ1*, *nmd3ΔNES1*, and *tif6-1* but not in the slow growing *src1Δ* strain. Nucleoplasmic retention of Rpl25p-eGFP in the thermosensitive *tif6-1* allele was seen after a shift to 37°C for 8 hr. Lower panels: corresponding phase contrasts.

(B) Location of Rpl25p-eGFP (green) in a *efl1Δ1* nucleus in comparison to the DsRed-Nop1p (nucle(ol)ar marker, red). Both pictures were also merged.

marker. In wild-type cells, DsRed-Nop1p exclusively localized to the nucleolus (data not shown). In *efl1Δ1*, the DsRed-Nop1p marker showed a typical nucle(ol)ar distribution while Rpl25p-eGFP accumulated throughout the entire nucleus (Figure 5B). This demonstrates that the nucleoplasmic accumulation of Rpl25p-eGFP detected in *efl1Δ1* strains is not simply due to the enlargement and/or fragmentation of the nucleolus. The same conclusion was reached for *tif6-1* (data not shown).

Finally, the homology of Efl1p to translation factors prompted us to test whether proteins directly involved in translation could also exhibit a 60S subunit export defect. To test this, the cellular distribution of Rpl25p-eGFP was analyzed in mutants impaired in the initiation of translation, i.e., *gcd1-501* and *sui2-1*, the mutant alleles of translation initiation factors eIF2Bγ and eIF2α respectively. None of them accumulated the ribosomal protein reporter construct in the nucleus (see Supplemental Figure S1 at http://www.molecule.org/cgi/content/full/8/6/1363/dc1).

In Strains Deficient for Efl1p, Nucle(ol)ar Tif6p Is Redistributed to the Cytoplasm

To test whether Tif6p shuttles between the nucleus and the cytoplasm, which would allow it to contact cytoplasmic Efl1p, the cellular distribution of Tif6p was analyzed both by subcellular fractionation and GFP fluorescence microscopy.

Nuclear and cytoplasmic fractions were prepared from total extracts of wild-type, *efl1Δ1*, and R1 strains and probed with an anti-Tif6p antibody. In agreement with previous studies (Sanvito et al. 1999; Wood et al. 1999), Tif6p was mainly found in the nuclear fraction in wild-type strains (Figure 6A). Strikingly, Tif6p was significantly recovered in the cytosolic fraction in the *efl1Δ1* strain, but has a wild-type distribution in the R1 suppressor strain. The results derived from these subcellular fractionation studies are fully supported by fluorescence microscopy analysis; GFP-Tif6p was only detected in the nucleus in wild-type cells, whereas it was completely mislocalized to the cytoplasm in *efl1Δ1* strains (Figure 6B). This suggests that Tif6p is a shuttling protein, whose steady-state distribution in the cell is dependent on Efl1p.

Efl1p Promotes the Dissociation of Tif6p-60S Complexes In Vitro

Although Efl1p could be involved in nuclear import of Tif6p, an attractive possibility is that GTP hydrolysis mediated by Efl1p triggers the release of Tif6p from 60S pre-ribosomes in the cytoplasm.

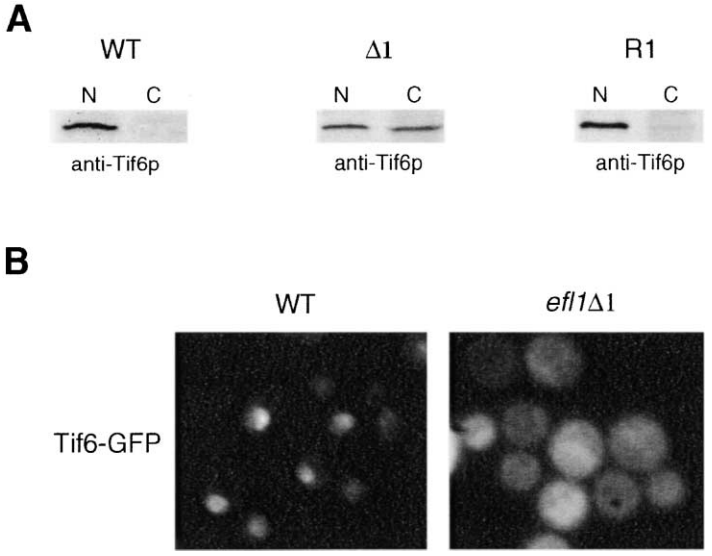

Figure 6. Subcellular Distribution of Tif6p in Wild-Type, *efl1Δ1*, and R1 Strains

(A) Cell fractionation. Crude cytosolic protein extract (lane C) from about 0.3 A_{600} cells were loaded on a 10% SDS-gel. Equivalent amounts of nuclear protein extracts were loaded on lane N. Tif6p was visualized using the ECL protocol (Amersham) and corresponding specific sera diluted 1/5000.

(B) Tif6p-GFP fluorescence signal in live cells of wild-type and *efl1Δ1* strains.

To test this hypothesis, 40S and 60S subunits, isolated from a wild-type strain, were incubated with recombinant Tif6p either in the presence or absence of recombinant Efl1p, and their capability to form 80S ribosomes was monitored by sucrose gradient centrifugation. The rationale was that any displacement of Tif6p from 60S (Tif6p was originally identified by virtue of its antiassociation activity [Si and Maitra, 1999]) should induce the formation of 80S particles.

Consistent with this possibility, we found that in the presence of Efl1p and GTP, formation of 80S ribosomes was increased by 20% with a concomitant reduction of 60S-bound Tif6p (Figure 7A, compare fractions 17–20 in the absence and presence of Efl1p) and a noticeable elevation in the level of free Tif6p at the top of the gradient (Figure 7A, fractions 27–30). The distribution of Tif6p in the gradient relative to Rpl25p was quantitated from the Western blots. The ratio of Tif6p versus Rpl25p varied from 1.75–2.3 in the absence of Efl1p to 0.6–1.0 in the presence of the protein. We conclude that, in vitro, Efl1p promotes the dissociation of 60S-Tif6p complexes.

The GTPase Activity of Efl1p Is Stimulated by 60S Subunits

To establish that Efl1p is a bona fide GTPase, purified recombinant protein was incubated with [γ^{32}P]-GTP and the products of the reaction resolved by thin layer chromatography. Efl1p showed weak but reproducible GTPase activity (Figure 7B, compare lanes 1 and 2). GTPases often show limited intrinsic activity that is stimulated several fold by associated factors. For ribosomal translocases, stimulation is provided by an integral part of the large ribosomal subunit, the so-called GTPase-associated region (Wimberly et al. 1999). To test whether Efl1p is also prone to stimulation by the ribosome, the GTPase assay was repeated in the presence of purified 60S subunits (Figure 7B, lanes 3–5). Even though 60S subunits were extensively washed in high salt and magnesium (as described in Zurdo et al. 2000), background GTPase activity was detected in the absence of Efl1p (Figure 7B, lane 3). This is due to the residual level of associated EF-2. The addition of 60S subunits to Efl1p stimulated its GTPase activity 34-fold (Figures 7B and 7C, lanes 2 and 4). This stimulation was dependent on the amount of enzyme used in this assay (Figures 7B and 7C, lanes 4 and 5). The activity of Efl1p was not further stimulated when 80S ribosomes were used in place of 60S subunits. This is as previously described for EF-2 (Nygard and Nilsson, 1989, 1990). We propose that Efl1p is a GTPase whose activity is stimulated by the ribosome.

Discussion

In this work, we describe the identification and functional characterization of Efl1p, a G-domain containing protein involved in ribosome synthesis. Efl1p is homologous to the ribosomal translocases EF-G/EF-2 and shares many conserved features with this family of proteins including the domain G itself which is known to be involved in GTP binding and hydrolysis (Berchtold et al. 1993; Czworkowski et al. 1994). Consistent with this, recombinant Efl1p was found to be capable of hydrolyzing GTP in vitro, and this activity was stimulated several fold in the presence of 60S ribosomal subunits or 80S ribosomes.

Efl1p is not essential but required for optimal growth. Strains deleted for Efl1p (*efl1Δ1*) show reduced levels of polyribosomes and underaccumulate 60S ribosomal subunits. Pre-rRNA processing analysis revealed that *efl1*-deficient strains are inhibited for the synthesis of 5.8S and 25S rRNAs, two RNA components of the large ribosomal subunit. In addition, strains deficient for Efl1p were delayed for early nucle(ol)ar cleavages at sites A_0–A_2, leading to a strong accumulation of the aberrant 23S RNA. Many strains affected for the synthesis of the large ribosomal subunit rRNAs show similar feed-back inhibitions on cleavages at sites A_0–A_2. This is believed to be part of a quality control mechanism and suggests high levels of coordination between protein complexes

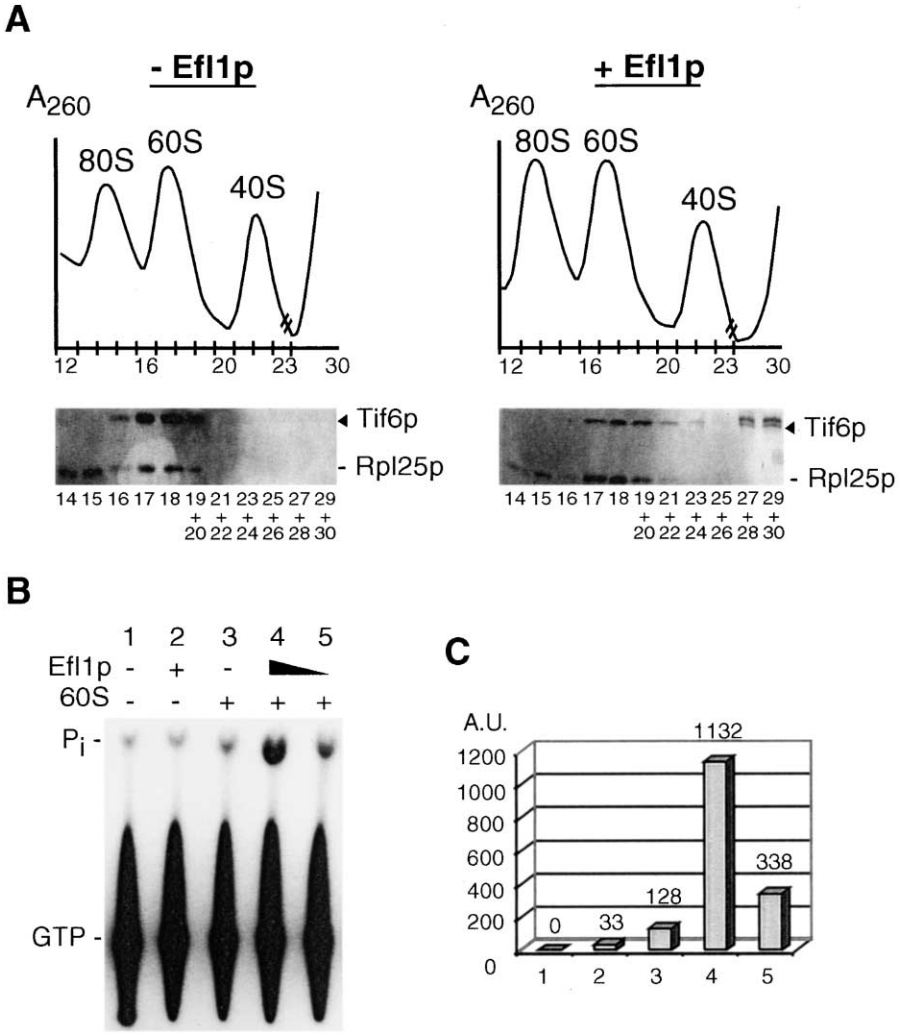

Figure 7. In Vitro Release of Tif6p and Ribosome-Dependent GTPase Activity of Efl1p

(A) Reconstitution of 80S in vitro in the presence and absence of GST-Efl1p. Formation of 80S ribosomes from isolated 60S and 40S subunits was analyzed by sucrose gradient centrifugation. Each individual fraction of the 80S and 60S peak was analyzed by Western blotting using anti-GST-Tif6p and Rpl25 antibodies. Pools of two fractions were analyzed after fraction 18. The two last lanes correspond to the top fractions of the gradient. In these fractions, the upper band revealed by the GST-Tif6p antibodies corresponded to GST released from the GST-Efl1p fusion.

(B) GTPase activity of GST-Efl1p analyzed by thin-layer chromatography. 60S obtained from run-off ribosomes were washed and centrifuged as described in Zurdo et al. (2000). The pelleted material was suspended in the buffer used to test the GTPase activity. 60S subunits (0.5 pmol) were incubated in the presence of GST-Efl1p and 2 μM [γ^{32}P] GTP for 1 hr at 25°C. Lane 1 (control of the GTP hydrolysed), lane 2 (intrinsic GTPase activity of GST-Efl1p), lane 3 (endogeneous GTPase activity of the 60S) enzymatic GTPase activity of GST-Efl1p obtained with 0.125 and 0.5 pmol of GST-Efl1p. The position of Pi resulting from [γ^{32}P] GTP hydrolysis is indicated. The data were quantified after having substracted the blank value measured in lane 1. A.U. stands for arbitrary units.

at work at distant sites on the pre-rRNAs (for further discussion see Venema and Tollervey, 1999).

The fact that Efl1p could only be detected in the cytoplasm, points to an indirect role in nucle(ol)ar pre-rRNA processing and suggests an involvement in a late cytoplasmic maturation step of the 60S subunits biogenesis.

Genetic studies led to the identification of Tif6p as an extragenic suppressor of *efl1Δ1* strains. Tif6p is an essential nucle(ol)ar protein stably associated with 60S subunits and required for 5.8S and 25S pre-rRNA processing (Basu et al. 2001). The slow growth phenotype of *efl1Δ1* was suppressed by a single substitution in Tif6p (tif6* allele) and partially complemented by mild overexpression of wild-type Tif6p. Pre-rRNA processing defects reported in *tif6* and *efl1* mutants are very similar; in addition, both *efl1* and *tif6* mutants are defective for nuclear export of 60S subunits. However, the accumulation of Tif6p was not affected in strains deleted for Efl1p. In fact the two proteins could not be detected in association either in vivo or in vitro and were present in distinct cellular compartments at steady state (Sanvito et al. 1999; Wood et al. 1999; and this work). Remarkably, in the absence of Efl1p, Tif6p became mislocalized to the cytoplasm. This finding offers an explanation as to how Tif6p, a nucle(ol)ar protein, participates in the assembly of 60S subunits and shows ribosome antiassociation activity in vitro (Si and Maitra, 1999).

Given the fact that Tif6p-60S complexes are dissoci-

ated in vitro in the presence of Efl1p, we suggest that in the course of ribosomal assembly, Tif6p binds to the pre-ribosomes in the nucle(ol)us and escorts them through the NPC into the cytoplasm where a structural rearrangement mediated by Efl1p facilitates the release of Tif6p from 60S and its recycling to the nucle(ol)us. In this process, Efl1p acts as a catalyst, i.e., spontaneous release of Tif6p can occur (indeed, *EFL1* is not essential). However, in the absence of Efl1p, dissociation of the complex would become rate limiting, and Tif6p would progressively be depleted from the nucle(ol)us with concomitant inhibition of pre-rRNA processing and ribosome export. In Tif6p*, the single V192F substitution would weaken the interaction of the protein with pre-ribosomes, and a sufficient amount of Tif6p would be provided to the pre-rRNA processing machinery even in the absence of the optimal recycling normally mediated by Efl1p. Similarly, Tif6p overexpression would palliate limiting amounts of Tif6p in the nucle(ol)us. The demonstration that Tif6p is part of a late pre-60S particle ready to be exported is consistent with our model.

Passage of large RNPs, such as pre-ribosomes, through the NPC is likely to be preceded and followed by major structural rearrangements and the concomitant release of RNP-associated proteins, including processing and assembly factors. This presumably requires a considerable input of energy. In mature ribosomes, translocases act as force-generating motor proteins utilizing the energy from GTP hydrolysis to promote a series of synchronized molecular movements (Rodnina et al. 1999). By analogy, we propose that the energy provided by Efl1p-mediated GTP-hydrolysis is used for a late cytoplasmic structural rearrangement in the pre-ribosomes.

The overall homology of Efl1p to ribosomal translocases further suggests that their binding sites on the ribosome are conserved. If so, the association of Efl1p with cytoplasmic pre-ribosomes could provide a quality control step to check that the binding sites for elongation factors are properly shaped on mature subunits before they engage in translation. It seems likely that additional ribosomal RNA processing factors are released during late structural rearrangements in the cytoplasm that convert the pre-ribosomal particles to the mature ribosomal subunits. Failures in the reorganization of the pre-ribosomes and the consequent deficit in the recycling of processing factors may underlie the long-standing observation that many mutations leading to the underaccumulation of cytoplasmic 60S subunits also inhibit early pre-rRNA processing reactions.

Experimental Procedures

Purification of Recombinant GST-Tif6p and GST- Efl1p

Efl1p and Tif6p were cloned by PCR in pGEX-4T-3 (APBiotech, Orsay, France) to yield GST-Efl1p and GST-Tif6p, respectively, and purified following the instructions of the manufacturer.

GTPase Assay

Purified recombinant GST-Efl1p (0.125 and 0.5 pmol) was incubated at 28°C for 45 min in a buffer containing 20 mM Tris-HCl (pH 7.5), 30 mM NH_4Cl, 15 mM $MgCl_2$, 2 μM GTP, and 0.5 pmol 60S subunits. The [γ^{32}P] GTP (NEN Life Science, Zaventem, Belgium) was diluted to a final specific activity of 12 kdpm per pmol in the assay. The inorganic phosphate (Pi) released upon cleavage of GTP was analyzed by thin layer chromatography on PEI-cellulose sheets and quantitated with a Fuji phosphor-imager.

GFP Fluorescence Microscopy

The GFP signal of various tagged proteins was examined in the fluorescein (for GFP fusions) or rhodamine (for DsRed) channels of a Zeiss Axioskop fluorescence microscope. Pictures were obtained with a Xillix Microimager CCD camera and processed with Improvision (Open lab) and Photoshop 4.0.1 (Adobe).

RNA Analyses

10 μg of total RNA were extracted from *efl1Δ1* and wild-type strains grown in complete medium. Total RNA was either separated on 1.2% agarose-formaldehyde or 8% polyacrylamide gels and processed for primer extension as previously described (Lafontaine et al., 1995). Oligonucleotide specific to 5S rRNA was CTACTCGGT CAGGCTC. Other oligonucleotide probes used in this study were described previously (Lafontaine et al. 1995). Pulse-chase analysis was performed according to Lafontaine et al. (1995).

Genetic Analysis

One copy of *EFL1* in the diploid strain YPH501 was disrupted by the HIS3 marker as indicated in Results. Efl1 disruption at the correct chromosomal locus was verified by Southern blotting. Disrupted alleles from YPH501 were crossed to S288c derivative strain FY1361. Segregants from this cross were used to obtain haploid *efl1Δ1* strains with complementing markers (JS544-6A and JS544-8D) and to construct homozygous diploid deletants. The slow growth phenotype of *efl1Δ1* strain does not change after outcrossing of the disrupted allele into a different genetic background. Revertants were obtained from strain JS544-6A as colonies visible after two days of growth and termed R1–R5. Diploids, obtained by crossing each of them to JS544-8D were used to test whether the revertant loci were dominant or recessive with respect to the *efl1Δ1* allele. DNA from the R1 strain was used to construct aDNA library, which was introduced into strain JS544-6A. Transformants were screened for wild-type growth.

In Vitro Reconstitution of 80S Ribosomes

Free 60S and 40S subunits recovered from polyribosomes of cycloheximide-arrested wild-type cells were pelleted by centrifugation at 45,000 rpm for 14 hr in a Beckman TI50 rotor and resuspended in the appropriate buffer to follow the formation of 80S (50 mM KCl and 5 mM $MgCl_2$). 23 pmol of each subunit were incubated in the absence and presence of 23 pmol of GST-Efl1p and 1mM GTP for 45 min at 30°C. The 80S formed were analyzed on 10%–30% sucrose gradients run for 3.5 hr at 37,000 rpm in a SW41 rotor.

Acknowledgments

We thank Prof. H. Trachsel (University of Bern) for fruitful discussions and suggestions and J. Bassler (University of Heidelberg) for providing us the Western blot with Noc1p, Noc3p, and Tif6p. We acknowledge the excellent technical assistance of Gaby Nussbaum. D.L.J.L. is a Chercheur qualifié du Fond National de la Recherche Scientifique Belge (F.N.R.S). E.C.H. is recipient of grants from the Deutsche Forschungsgemeinschaft (Schwerpunktprogramm "Funktionelle Architektur des Zellkerns") and O.G. was a holder of a HFSP fellowship. This work was supported by grants from the Association pour la Recherche sur le Cancer (ARC) and from the CNRS.

Received July 17, 2001; revised October 18, 2001.

References

Aevarsson, A.J. (1995). Structure-based sequence alignment of elongation factors Tu and G with related GTPases involved in translation. J. Mol. Evol. *41*, 1096–1104.

Aevarsson, A., Brazhnikov, E., Garber, M., Zheltonosova, J., Chirgadze, Y., al-Karadaghi, S., Svensson, L.A., and Liljas, A. (1994). Three-dimensional structure of the ribosomal translocase: elongation factor G from Thermus thermophilus. EMBO J. *13*, 3669–3677.

Basu, U., Si, K., Warner, J.R., and Maitra, U. (2001). The *Saccharo-*

myces cerevisiae TIF6 gene encoding translation initiation factor 6 is required for 60S ribosomal subunit biogenesis. Mol. Cell. Biol. *21*, 1453–1462.

Bassler, J., Grandi, P., Gadal, O., Lessmann, T., Petfalski, E., Tollervey, D., Johannes Lechner, J., and Hurt, E. (2001). Identification of a 60S pre-ribosomal particle that is closely linked to nuclear export. Mol. Cell, *8*, 517–529.

Bataille, N., Helser, T., and Fried, H.M. (1990). Cytoplasmic transport of ribosomal subunits microinjected into the Xenopus laevis oocyte nucleus: a generalized, facilitated process. J. Cell Biol. *111*, 1571–1582.

Berchtold, H., Reshetnikova, L., Reiser, C.O., Schirmer, N.K., Sprinzl, M., and Hilgenfeld, R. (1993). Crystal structure of active elongation factor Tu reveals major domain rearrangements. Nature *365*, 126–132.

Czworkowski, J., Wang, J., Steitz, T.A., and Moore, P.B. (1994). The crystal structure of elongation factor G complexed with GDP at 2.7 Å resolution. EMBO J. *13*, 3661–3668.

de la Cruz, J., Kressler, D., and Linder, P. (1999). Unwinding RNA in *Saccharomyces cerevisiae*: DEAD-box proteins and related families. Trends Biochem. Sci. *24*, 192–198.

Fabrizio, P., Laggerbauer, B., Lauber, J., Lane, W.S., and Lührmann, R. (1997). An evolutionarily conserved U5 snRNP-specific protein is a GTP-binding factor closely related to the ribosomal translocase EF-2. EMBO J. *16*, 4092–4106.

Gadal, O., Strauss, D., Kessl, J., Trumpower, B., Tollervey, D., and Hurt, E. (2001). Nmd3p functions as a nuclear adaptor for Xpo1p-dependent export of 60S ribosomal subunits. Mol. Cell. Biol. *21*, 3405–3415.

Galy, V., Olivo-Marin, J.C., Scherthan, H., Doye, V., Rascalou, N., and Nehrbass, U. (2000). Nuclear pore complexes in the organization of silent telomeric chromatin. Nature *403*, 108–112.

Ho, J., Kallstrom, G., and Johnson, A.J. (2000). Nmd3p is a Crm1p-dependent adapter protein for nuclear export of the large ribosomal subunit. J. Cell Biol. *151*, 1057–1066.

Hurt, E., Hannus, S., Schmelzl, B., Lau, D., Tollervey, D., and Simos, G. (1999). A novel *in vivo* assay reveals inhibition of ribosomal nuclear export in ran-cycle and nucleoporin mutants. J. Cell Biol. *144*, 389–401.

Kressler, D., Linder, P., and de la Cruz, J. (1999). Protein trans-acting factors involved in ribosome biogenesis in *Saccharomyces cerevisiae*. Mol. Cell. Biol. *19*, 7897–7912.

Lafontaine, D.L., and Tollervey, D. (1998). Birth of the snoRNPs: the evolution of the modification-guide snoRNAs. Trends Biochem. Sci. *23*, 383–388.

Lafontaine, D.L., and Tollervey, D. (2001). The function and synthesis of ribosomes. Nat. Rev. Mol. Cell. Biol. *2*, 514–520.

Lafontaine, D.L., Vandenhaute, J., and Tollervey, D. (1995). The 18S rRNA dimethylase Dim1p is required for pre-ribosomal RNA processing in yeast. Genes Dev. *9*, 2470–2481.

Milkereit, P., Gadal, O., Podtelejnikov, A., Trumtel, S., Gas, N., Petfalski, E., Tollervey, D., Mann, M., Hurt, E., and Tschochner, H. (2001). Maturation and intranuclear transport of pre-ribosomes requires Noc proteins. Cell *105*, 499–509.

Moy, T.I., and Silver, P.A. (1999). Nuclear export of the small ribosomal subunit requires the ran-GTPase cycle and certain nucleoporins. Genes Dev. *13*, 2118–2133.

Nygard, O., and Nilsson, L. (1989). Characterization of the ribosomal properties required for formation of a GTPase active complex with elongation factor 2. Eur. J. Biochem. *179*, 603–609.

Nygard, O., and Nilsson, L. (1990). Translational dynamics. Interactions between the translational factors, tRNA and ribosomes during eukaryotic protein synthesis. Eur. J. Biochem. *191*, 1–17.

Raué, H.A., and Planta, R.J. (1991). Ribosome biogenesis in yeast. Prog. Nucleic Acid Res. Mol. Biol. *41*, 89–129.

Rodnina, M.V., Savelsbergh, A., and Wintermeyer, W. (1999). Dynamics of translation on the ribosome: molecular mechanics of translocation. FEMS Microbiol. Rev. *23*, 317–333.

Sanvito, F., Piatti, S., Villa, A., Bossi, M., Lucchini, G., Marchisio, P.C., and Biffo, S. (1999). The beta4 integrin interactor p27(BBP/eIF6) is an essential nuclear matrix protein involved in 60S ribosomal subunit assembly. J. Cell Biol. *144*, 823–837.

Si, K., and Maitra, U. (1999). The *Saccharomyces cerevisiae* homologue of mammalian translation initiation factor 6 does not function as a translation initiation factor. Mol. Cell. Biol. *19*, 1416–1426.

Si, K., Chaudhuri, J., Chevesich, J., and Maitra, U. (1997). Molecular cloning and functional expression of a human cDNA encoding translation initiation factor 6. Proc. Natl. Acad. Sci. USA *94*, 14285–14290.

Trapman, J., and Planta, R.J. (1976). Maturation of ribosomes in yeast. Biochim. Biophys. Acta *442*, 265–274.

Venema, J., and Tollervey, D. (1999). Ribosome synthesis in *Saccharomyces cerevisiae*. Annu. Rev. Genet. *33*, 261–311.

Warner, J.R. (1971). The assembly of ribosomes in yeast. J. Biol. Chem. *246*, 447–454.

Warner, J.R. (1999). The economics of ribosome biosynthesis in yeast. Trends Biochem. Sci. *24*, 437–440.

Wimberly, B.T., Guymon, R., McCutcheon, J.P., White, S.W., and Ramakrishnan, V. (1999). A detailed view of a ribosomal active site: the structure of the L11-RNA complex. Cell *97*, 491–502.

Woolford. J.L., Jr, and Warner, J.R. (1991). The ribosome and its synthesis. In The Molecular and Cellular Biology of the Yeast Saccharomyces: Genome Dynamics, Protein Synthesis and Energetics, Broach, J.R., Pringle, J.R., and Jones, E.W., ed. (Cold Spring Harbor, NY: Cold Spring Harbor Laboratory Press), pp. 587–625.

Wood, L.C., Ashby, M.N., Grunfeld, C., and Feingold, K.R. (1999). Cloning of murine translation initiation factor 6 and functional analysis of the homologous sequence YPR016c in *Saccharomyces cerevisiae*. J. Biol. Chem. *274*, 11653–11659.

Zurdo, J., Parada, P., van den Berg, A., Nusspaumer, G., Jimenez-Diaz, A., Remacha, M., and Ballesta, J.P. (2000). Assembly of *Saccharomyces cerevisiae* ribosomal stalk: binding of P1 proteins is required for the interaction of P2 proteins. Biochemistry *39*, 8929–8934.